

UCID--20577

DE86 008148

A PRELIMINARY EVALUATION OF NEUTRON CAPTURE
CROSS SECTIONS FOR ^{144}SM , ^{145}SM AND ^{145}PM

D. G. Gardner
M. A. Gardner

February 13, 1986

The logo for Lawrence Livermore National Laboratory, featuring a stylized 'L' symbol and the text 'Lawrence Livermore National Laboratory' arranged in a V-shape.

Lawrence
Livermore
National
Laboratory

This is an informal report intended primarily for internal or limited external distribution. The opinions and conclusions stated are those of the author and may or may not be those of the Laboratory.

Work performed under the auspices of the U.S. Department of Energy by the Lawrence Livermore Laboratory under Contract W-7405-Eng-48.

A PRELIMINARY EVALUATION OF NEUTRON CAPTURE
CROSS SECTIONS FOR ^{144}Sm , ^{145}Sm AND ^{145}Pm

ABSTRACT

We have made preliminary neutron-capture cross-section calculations of the Hauser-Feshbach type for the isotopes ^{144}Sm , ^{145}Sm , and ^{145}Pm to investigate the production of radioactive ^{145}Pm by neutron capture on the stable isotope ^{144}Sm . The calculations were made for incident neutron energies from 2.5 MeV to about 10^{-4} or 10^{-5} MeV, wherever the first unbound resonance was estimated to occur in each case. At that energy, the calculated value was reduced by a somewhat arbitrary factor, and the excitation function extended down to thermal energy using a $(E_n)^{-1/2}$ energy dependence. Since very large uncertainties are associated with the position and magnitude of the first unbound resonance and the subsequent extrapolation back to thermal energy, the cross sections in this low-energy region should not be considered more accurate than \pm a factor of 10. For incident neutron energies above each step, the calculations represent an average through the separated and overlapping resonance regions and may be accurate to better than \pm a factor of 2.

INTRODUCTION AND SUMMARY

The 17.7-year radioactive isotope ^{145}Pm can be produced by neutron capture on the stable isotope ^{144}Sm , yielding ^{145}Sm which, in turn, decays by electron capture with a 340-day half life to ^{145}Pm . Figure 1 shows the isotopes¹ in the mass region of interest. Competing with electron-capture decay of ^{145}Sm is neutron capture to the long-lived ^{146}Sm isotope. Since the ^{145}Pm itself may be destroyed by neutron capture, it is necessary to estimate the neutron-capture cross sections that destroy ^{145}Sm and ^{145}Pm , as well as the capture cross sections that form ^{145}Sm from stable ^{144}Sm . Neutron capture on the other stable samarium isotopes produce either long-lived or stable daughter products, or samarium isotopes that beta decay to isotopes of europium. The only major isotope of promethium that will be produced is ^{145}Pm , together with possibly very small amounts of heavier promethium isotopes produced by successive neutron capture, depending on the details of

MASTER

DISTRIBUTION OF THIS DOCUMENT IS UNLIMITED ^{EP}

DISCLAIMER

This report was prepared as an account of work sponsored by an agency of the United States Government. Neither the United States Government nor any agency thereof, nor any of their employees, makes any warranty, express or implied, or assumes any legal liability or responsibility for the accuracy, completeness, or usefulness of any information, apparatus, product, or process disclosed, or represents that its use would not infringe privately owned rights. Reference herein to any specific commercial product, process, or service by trade name, trademark, manufacturer, or otherwise does not necessarily constitute or imply its endorsement, recommendation, or favoring by the United States Government or any agency thereof. The views and opinions of authors expressed herein do not necessarily state or reflect those of the United States Government or any agency thereof.

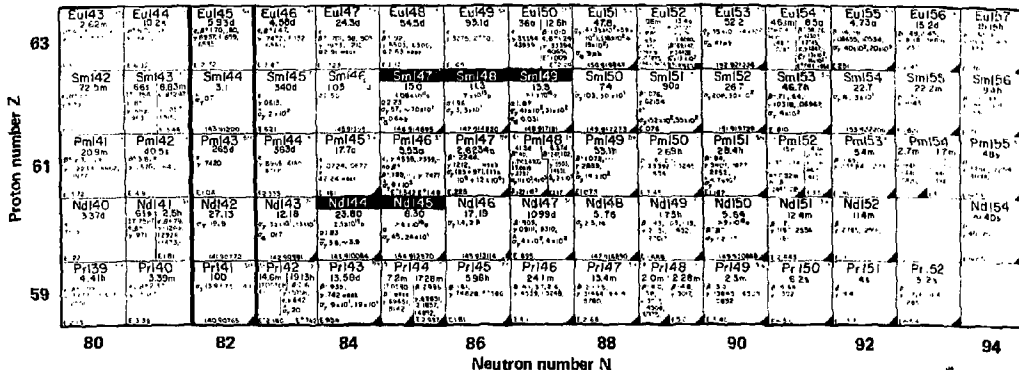


Figure 1. Nuclides in the Sm-Pm mass region.

the neutron irradiation. Its separation from samarium and europium should not present special problems.

Our calculated results are shown in Fig. 2 and tabulated in Table 1. The step decrease in each excitation function occurs at our estimate of the probable position of the first unbound resonance. We take this to be half of the average s-wave neutron resonance spacing, D_{ob} . For incident neutron energies above the step, the curves are the results of our Hauser-Feshbach-type calculations. For energies below the step, the curves are $(E_n)^{-1/2}$ extrapolations back to thermal energy. The magnitude of the step decrease was taken to be the same for all curves and was determined by requiring the ^{144}Sm cross section to extrapolate back to a value of 0.7 b (Ref. 2) at 2.54×10^{-8} MeV. There are very large uncertainties associated with the position and magnitude of each step and the subsequent extrapolation back to thermal energy; cross sections in this low-energy region should not be considered more accurate than \pm a factor of 10. For incident-neutron energies above each step, the calculations represent an average through the separated and overlapping resonance regions. They are certainly more reliable than the low-energy estimates and may be accurate to better than \pm a factor of 2. We discuss this error estimate later in this report.

Neutron-capture cross sections at or near thermal energy have been reported³ for a number of samarium isotopes. In some cases, these cross sections are "2200 m/sec" thermal energy values; in other cases, they are cross-section values averaged over a Maxwellian or other reactor distribution of neutron energies. These "thermal" values are shown in Table 2.

From Table 2 and Fig. 2, it is clear that thermal neutrons in particular and low-energy neutrons in general should be avoided as much as possible. If a reactor is chosen as the neutron source, we suggest that target sample positions be chosen to minimize the scattered and thermalized-neutron fluence and to maximize the fast-neutron fluence associated with a pure-fission neutron spectrum. A typical example⁵ of such a spectrum is shown in Fig. 3. This is the neutron spectrum produced by the thermal-neutron fission of ^{235}U . Also, the target samples probably should be wrapped in cadmium foil or some other thermal-neutron absorber to further decrease the production of undesired isotopes. Additional refinements might be considered, such as enriching the samarium target sample in ^{144}Sm or continuously recycling the samarium target material and concurrently removing the ^{145}Pm that is produced.

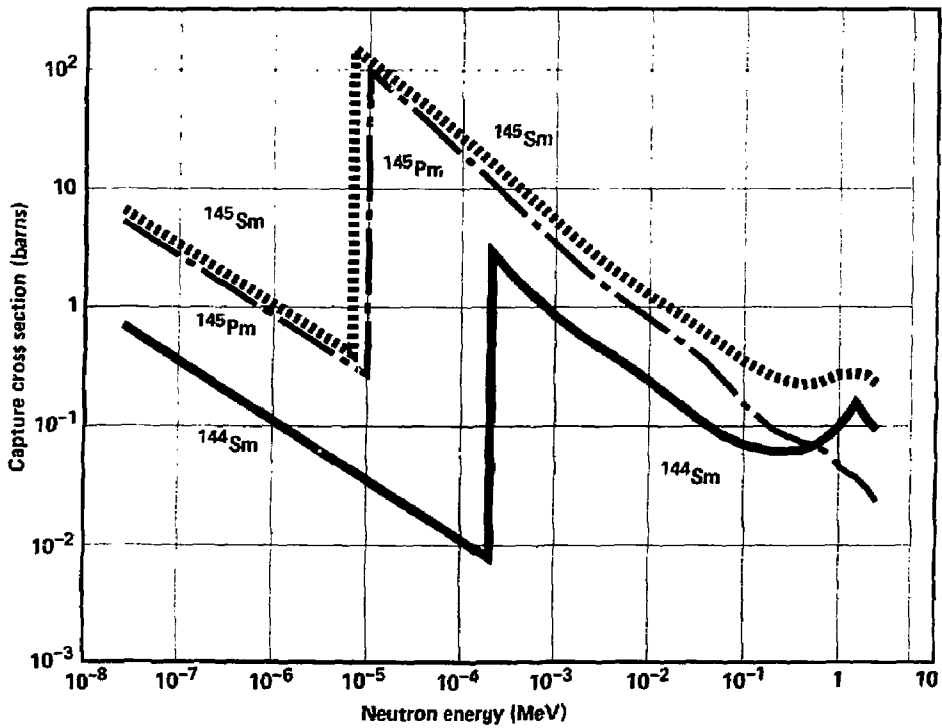


Figure 2. Calculated neutron-capture cross sections for ^{144}Sm , ^{145}Sm , and ^{145}Pm .

Table 1. Calculated neutron-capture cross sections.

^{144}Sm		^{145}Pm		^{145}Sm	
E(MeV)	$\sigma(\text{b})$	E(MeV)	$\sigma(\text{b})$	E(MeV)	$\sigma(\text{b})$
2.54×10^{-8}	7.00×10^{-1}	2.54×10^{-8}	5.31	2.54×10^{-8}	6.63
4.00×10^{-8}	5.58×10^{-1}	4.00×10^{-8}	4.23	4.00×10^{-8}	5.29
7.00×10^{-8}	4.22×10^{-1}	7.00×10^{-8}	3.20	7.00×10^{-8}	4.00
1.00×10^{-7}	3.53×10^{-1}	1.00×10^{-7}	2.68	1.00×10^{-7}	3.34
2.00×10^{-7}	2.50×10^{-1}	2.00×10^{-7}	1.89	2.00×10^{-7}	2.36
4.00×10^{-7}	1.76×10^{-1}	4.00×10^{-7}	1.34	4.00×10^{-7}	1.67
7.00×10^{-7}	1.33×10^{-1}	7.00×10^{-7}	1.01	7.00×10^{-7}	1.26
1.00×10^{-6}	1.12×10^{-1}	1.00×10^{-6}	8.46×10^{-1}	1.00×10^{-6}	1.06
2.00×10^{-6}	7.89×10^{-2}	2.00×10^{-6}	5.98×10^{-1}	2.00×10^{-6}	7.48×10^{-1}
4.00×10^{-6}	5.58×10^{-2}	4.00×10^{-6}	4.23×10^{-1}	4.00×10^{-6}	5.29×10^{-1}
7.00×10^{-6}	4.22×10^{-2}	7.00×10^{-6}	3.20×10^{-1}	6.90×10^{-6}	4.03×10^{-1}
1.00×10^{-5}	3.53×10^{-2}	1.00×10^{-5}	2.68×10^{-1}	7.00×10^{-6}	1.47×10^2
2.00×10^{-5}	2.49×10^{-2}	1.02×10^{-5}	9.78×10^1	1.00×10^{-5}	1.19×10^2
4.00×10^{-5}	1.76×10^{-2}	2.00×10^{-5}	6.16×10^1	2.00×10^{-5}	7.80×10^1
7.00×10^{-5}	1.33×10^{-2}	4.00×10^{-5}	3.80×10^1	4.00×10^{-5}	5.02×10^1
1.00×10^{-4}	1.12×10^{-2}	7.00×10^{-5}	2.54×10^1	7.00×10^{-5}	3.48×10^1
2.00×10^{-4}	7.89×10^{-3}	1.00×10^{-4}	1.96×10^1	1.00×10^{-4}	2.74×10^1
2.10×10^{-4}	2.88	2.00×10^{-4}	1.16×10^1	2.00×10^{-4}	1.69×10^1
4.00×10^{-4}	1.64	4.00×10^{-4}	6.85×10^1	4.00×10^{-4}	1.03×10^1
7.00×10^{-4}	1.09	7.00×10^{-4}	4.47	7.00×10^{-4}	6.92
1.00×10^{-3}	8.29×10^{-1}	1.00×10^{-3}	3.39	1.00×10^{-3}	5.31
2.00×10^{-3}	5.55×10^{-1}	2.00×10^{-3}	2.06	2.00×10^{-3}	3.26
4.00×10^{-3}	3.92×10^{-1}	4.00×10^{-3}	1.33	4.00×10^{-3}	2.08
7.00×10^{-3}	2.92×10^{-1}	7.00×10^{-3}	9.64×10^{-1}	7.00×10^{-3}	1.51
1.00×10^{-2}	2.39×10^{-1}	1.00×10^{-2}	7.92×10^{-1}	1.00×10^{-2}	1.25
2.00×10^{-2}	1.55×10^{-1}	2.00×10^{-2}	5.31×10^{-1}	2.00×10^{-2}	8.74×10^{-1}
3.00×10^{-2}	1.21×10^{-1}	4.00×10^{-2}	3.44×10^{-1}	3.00×10^{-2}	7.00×10^{-1}
6.00×10^{-2}	8.37×10^{-2}	7.00×10^{-2}	2.16×10^{-1}	6.00×10^{-2}	4.69×10^{-1}
1.00×10^{-1}	7.01×10^{-2}	1.00×10^{-1}	1.52×10^{-1}	1.00×10^{-1}	3.53×10^{-1}
2.00×10^{-1}	6.07×10^{-2}	2.00×10^{-1}	9.39×10^{-2}	2.00×10^{-1}	2.60×10^{-1}
4.00×10^{-1}	6.22×10^{-2}	4.00×10^{-1}	7.33×10^{-2}	4.00×10^{-1}	2.23×10^{-1}
6.00×10^{-1}	7.05×10^{-2}	6.00×10^{-1}	6.84×10^{-2}	6.00×10^{-1}	2.28×10^{-1}
8.00×10^{-1}	8.28×10^{-2}	8.00×10^{-1}	5.72×10^{-2}	8.00×10^{-1}	2.49×10^{-1}
1.00	9.90×10^{-2}	1.00	4.57×10^{-2}	1.00	2.69×10^{-1}
1.25	1.24×10^{-1}	1.25	4.03×10^{-2}	1.25	2.73×10^{-1}
1.50	1.55×10^{-1}	1.50	3.70×10^{-2}	1.50	2.78×10^{-1}
2.00	1.11×10^{-1}	2.00	2.99×10^{-2}	2.00	2.66×10^{-1}
2.50	9.28×10^{-2}	2.50	2.33×10^{-2}	2.50	2.25×10^{-1}

Table 2. "Thermal" neutron capture cross sections² of some samarium isotopes.

Target isotope	Cross section (barns)
Elemental Sm	5,670 \pm 100
¹⁴⁴ Sm	0.7 \pm 0.3 ^b
¹⁴⁵ Sm	\approx 220
¹⁴⁷ Sm	57 \pm 3 ^a
¹⁴⁸ Sm	2.4 \pm 0.6
¹⁴⁹ Sm	40,140 \pm 600 ^a
¹⁵⁰ Sm	104 \pm 4
¹⁵¹ Sm	15,200 \pm 300 ^a
¹⁵² Sm	206 \pm 6
¹⁵³ Sm	420 \pm 180 ^a
¹⁵⁴ Sm	8.4 \pm 0.5

^aThese are reported as "2200 m/sec" values.

^bRef. 4 gives a reactor-spectrum average absorption value of 0.03 b for ¹⁴⁴Sm.

In the following section, we discuss our Hauser-Feshbach calculations in more detail. The discussion will include comments on the choice of physics parameters used as input, comparison with some of the existing experimental data, and ways in which the calculations might be improved through additional work.

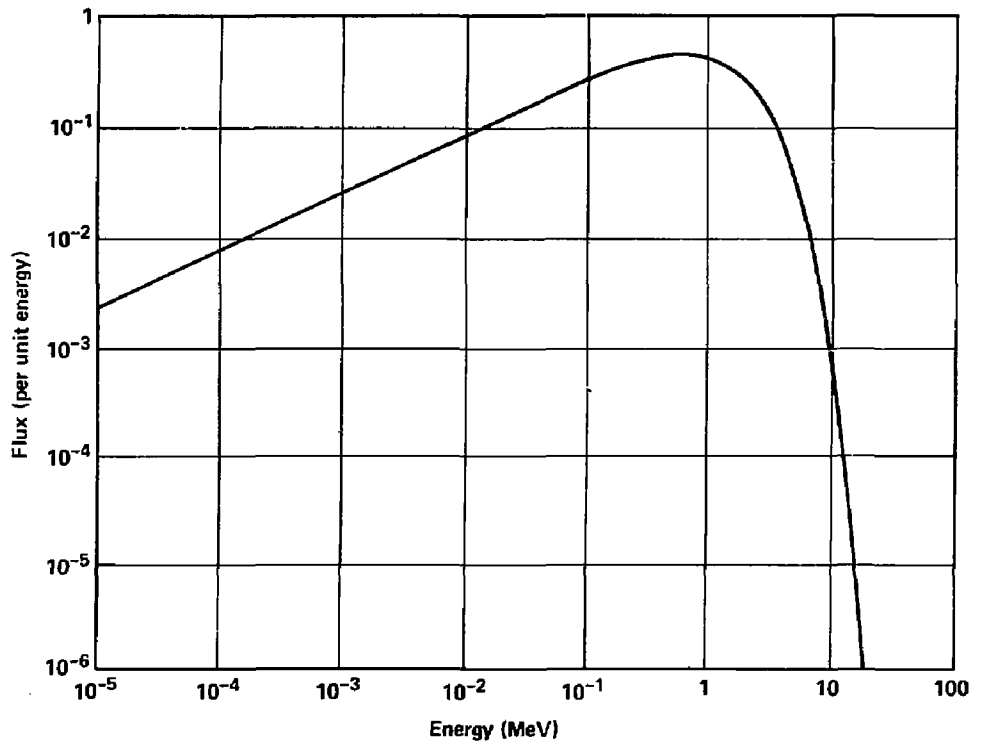


Figure 3. Thermal fission neutron spectrum for ^{235}U .

HAUSER-FESHBACH CALCULATIONS

The general approach to the calculation of neutron-capture cross sections using the Hauser-Feshbach method with the inclusion of width-fluctuation corrections is described in detail in Ref. 6. The computer codes that we used are our Nuclear Chemistry Division updated versions of STAPRE⁷ and COMMUC.⁸ Essentially, the problem is one of determining neutron and radiation widths and the nuclear level densities for a number of nuclei where few experimental data exist. From Fig. 1, we observe that the situation is further complicated by the fact that the target nucleus, ^{144}Sm , lies on the closed neutron shell at $N = 82$ but is some distance from any major proton shell. This produces a rather small neutron separation energy in ^{145}Sm and a general tendency for all of the samarium and promethium isotopes to rapidly become more deformed, with a concurrent increase in level densities as the neutron number increases. We show some relevant information in Table 3.

CHOICE OF PARAMETERS

The first choice to be made is that of a suitable neutron optical-model potential with which to generate the neutron transmission coefficients. We have chosen to try a spherical equivalent¹¹ of a deformed-nucleus potential for ^{169}Tm . At incident-neutron energies below a few tens of keV, the reaction is dominated by s-wave neutrons. In Table 4 are listed s-wave (S_0) and p-wave (S_1) neutron strength functions for some isotopes of samarium and promethium.

Similar S_0 and S_1 values are reported in Ref. 12 for some isotopes of neodymium, samarium, gadolinium, and erbium. We observe that our optical potential, derived for ^{169}Tm , does not reproduce the literature values for S_0 and S_1 very well. Below an incident-neutron energy of a few keV, our calculated total, reaction, and compound elastic cross sections may be too low. Figure 4 compares one of our calculated total cross sections with data from the BNL-325 compilation.¹³ Although our calculations tend to be low, the discrepancy is usually within 50% of the given data.

Another test of our optical potential involved the calculation of the total elastic cross section for the target isotope ^{147}Pm . The results are given in Fig. 5. The evaluated curve was constructed from resonance parameters (omitting two negative energy resonances) by Howerton.¹⁴ Again,

Table 3. Information related to level densities and radiation widths for some isotopes of samarium and promethium.

Compound nuclide	Neutron separation energy (MeV) ⁹	# of discrete levels ¹⁰ used in our calc.	Avg. s-wave Γ_{γ} (meV)		D_{ob} (eV)	
			Ref.3	Calc.	Ref.3	Calc.
¹⁴⁴ Sm	10.524	9				
¹⁴⁵ Sm	6.763	15		81		418
¹⁴⁶ Sm	8.400	18		95		14.6
¹⁴⁷ Sm	6.352					
¹⁴⁸ Sm	8.141		69 ± 2		5.7 ± 0.5	
¹⁴⁹ Sm	5.872					
¹⁵⁰ Sm	7.986		62 ± 2		2.2 ± 0.2	
¹⁵¹ Sm	5.597		60 ± 5		(55 ± 9) ^a	
¹⁵² Sm	8.258		92 ± 7		(1.2 ± 0.2) ^a	
¹⁵³ Sm	5.868		61 ± 7		(52 ± 3) ^a	
¹⁵⁴ Sm	7.968					
¹⁵⁵ Sm	5.814		79 ± 9		(115 ± 12) ^a	
¹⁴⁴ Pm	6.529					
¹⁴⁵ Pm	7.926	9				
¹⁴⁶ Pm	6.243	1		61		20.5
¹⁴⁷ Pm	7.670	7				
¹⁴⁸ Pm	5.902	3	68 ± 6	45	(3.6 ± 0.5) ^a	15.8
¹⁴⁹ Pm	7.265		80 ± 4			

^aSpins and parities of resonances were not identified.

Table 4. Some s-wave (S_0) and p-wave (S_1) neutron-strength functions for samarium and promethium.

Target nuclide	S_0 ($\times 10^4$)		S_1 ($\times 10^4$)	
	Ref.3	Calc.	Ref.3	Calc.
Elemental Sm	3.2 ± 0.4			
^{144}Sm	3.2 ± 1.4	1.07		2.42
^{145}Sm		1.08		2.39
^{147}Sm	4.8 ± 0.5			
^{148}Sm	3.8 ± 1.1		1.9 ± 0.2	
^{149}Sm	4.6 ± 0.6		0.3 ± 0.1	
^{150}Sm	3.6 ± 1.1		0.08 ± 0.02	
^{151}Sm	4.2 ± 0.4			
^{145}Pm		1.08		2.39
^{147}Pm		1.12		2.33

our calculation, which is the sum of the shape elastic and the compound elastic cross sections, tends to be low. Given the possible uncertainty in the resonance parameters, the agreement is not unsatisfactory. For example, had the two negative resonances been included in producing the evaluated curve, an average through the resonances would have exceeded the total cross section.

For the neutron-capture cross-section calculations described here, we used the absolute E1 and M1 gamma-ray strength functions previously obtained¹⁵ for ^{176}Lu . There remained to be determined the nuclear level density for each of the isotopes involved. We use the Gilbert-Cameron level density formalism, with parameters updated by Cook, et al.¹⁶ For an accurate calculation, we normalize these parameters to agree with the low-lying levels in each nucleus. Around closed shells, we may require the first 25 to 50 levels; for deformed nuclei, up to 1000 levels may be necessary. In Table 3 we show the number of discrete levels used for each nucleus in our calculations. This

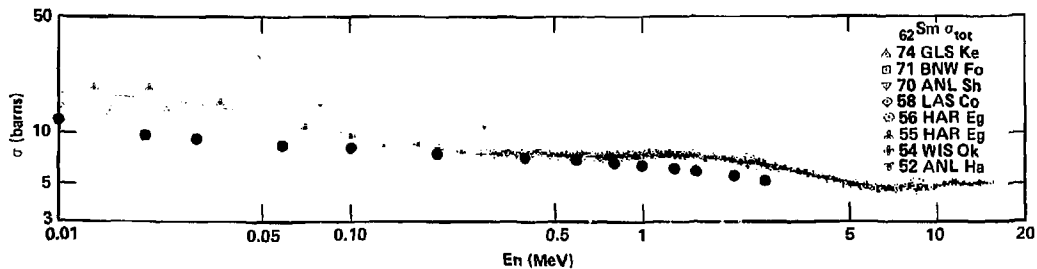
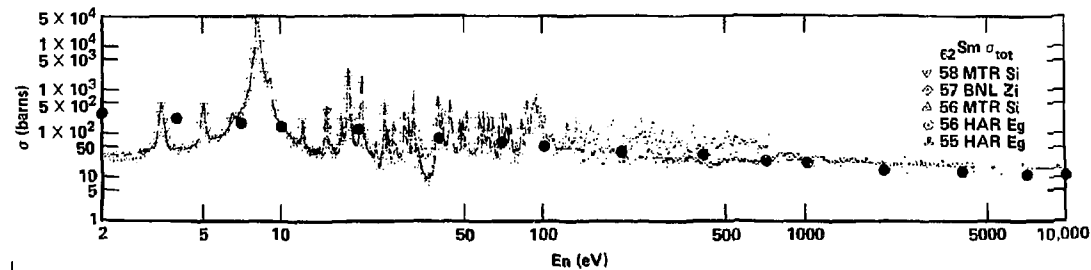


Figure 4. Experimental values for the total neutron cross section (σ) of elemental Sm, compared with calculated values (.) for the target isotope ^{145}Sm .

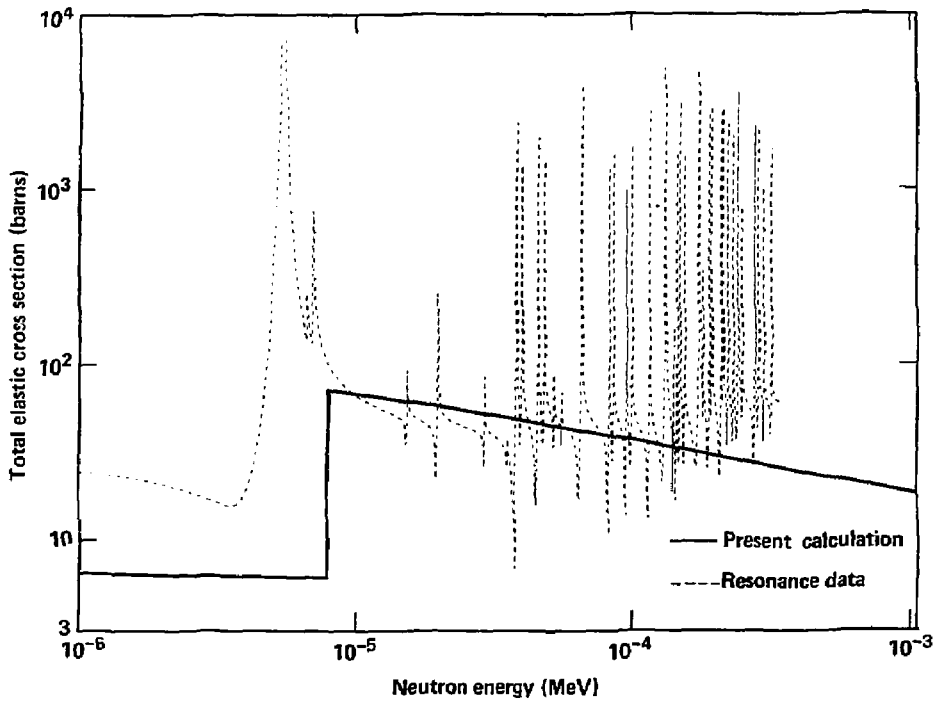


Figure 5. Calculated and experimental neutron total elastic scattering cross sections in the resonance region for ^{147}Pm (bound resonances excluded).

number ranges from 1 level (the ground state) for ^{146}Pm up to 18 levels for ^{146}Sm . None of these are adequate, and the quality of the level sets is unknown (particularly in regard to missing levels). Nevertheless, we have used the available levels for normalization purposes, except for ^{146}Pm and ^{148}Pm , where we guessed that there were about 17 levels up to 1 MeV in each nucleus. The level density and D_{ob} (and, thereby, the estimated position of the first resonance) can be quite sensitive to this normalization. For ^{145}Sm , as an example, the calculated D_{ob} changed by a factor of about 4 when the built-in parameters were adjusted to reproduce 15 levels up to 1.997 MeV. Since we choose the position of the first resonance to be $D_{ob}/2$, the position of the step decrease in the ^{144}Sm curve in Fig. 2 would change by the same factor.

Because we use absolute gamma-ray strength functions, our calculated radiation widths are not as sensitive to changes in the level densities as are the D_{ob} values. In the case just mentioned, the normalization caused only a 16% change in Γ_γ .

COMPARISON WITH SOME EXPERIMENTAL CAPTURE CROSS SECTIONS

We try to assess the accuracy of our calculated capture cross sections and our estimates of the position of the first resonance by comparison with experimental data where such are available. No ad hoc parameter adjustment was allowed. For ^{144}Sm neutron capture, some data have been measured.¹² In Fig. 6 we show the experimental and calculated cross sections from 1 keV to 2.5 MeV. For a calculation that was not adjusted post hoc to fit any cross-section measurements, the agreement is satisfactory.

Some neutron capture resonance data exist for ^{147}Pm . The constructed excitation function and a numerical average through the resonances¹⁴ is given in Fig. 7a. For comparison, we show in Fig. 7b our calculation with the step decrease where we estimated the first resonance to lie. The best that we can hope for from our Hauser-Feshbach calculations is a proper average through the resonance region, and we appear to have achieved this. There is no way to make a much better estimate as to where the first resonance lies, much less whether it is a large or small resonance. The position agreement shown in Fig. 7b is better than we expected it to be. The depth of the step decrease is meant to

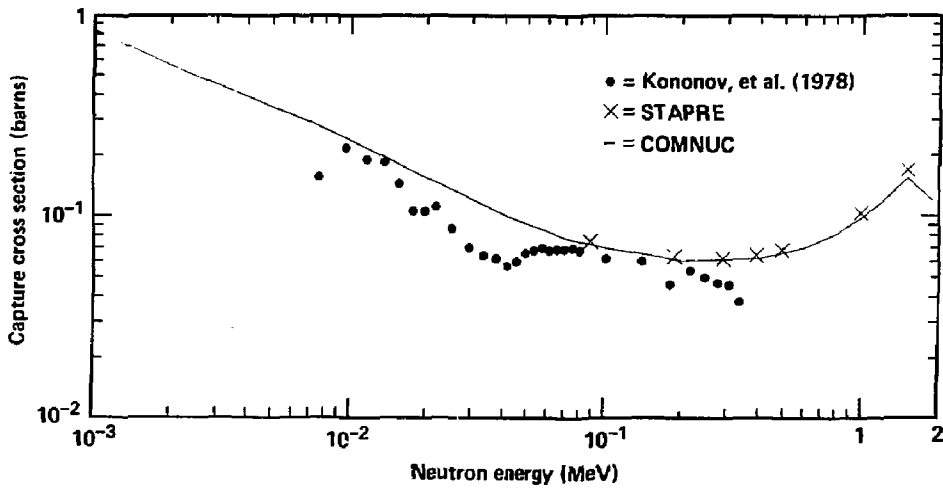


Figure 6. Comparison of calculated and experimental values for the ^{144}Sm neutron-capture excitation function.

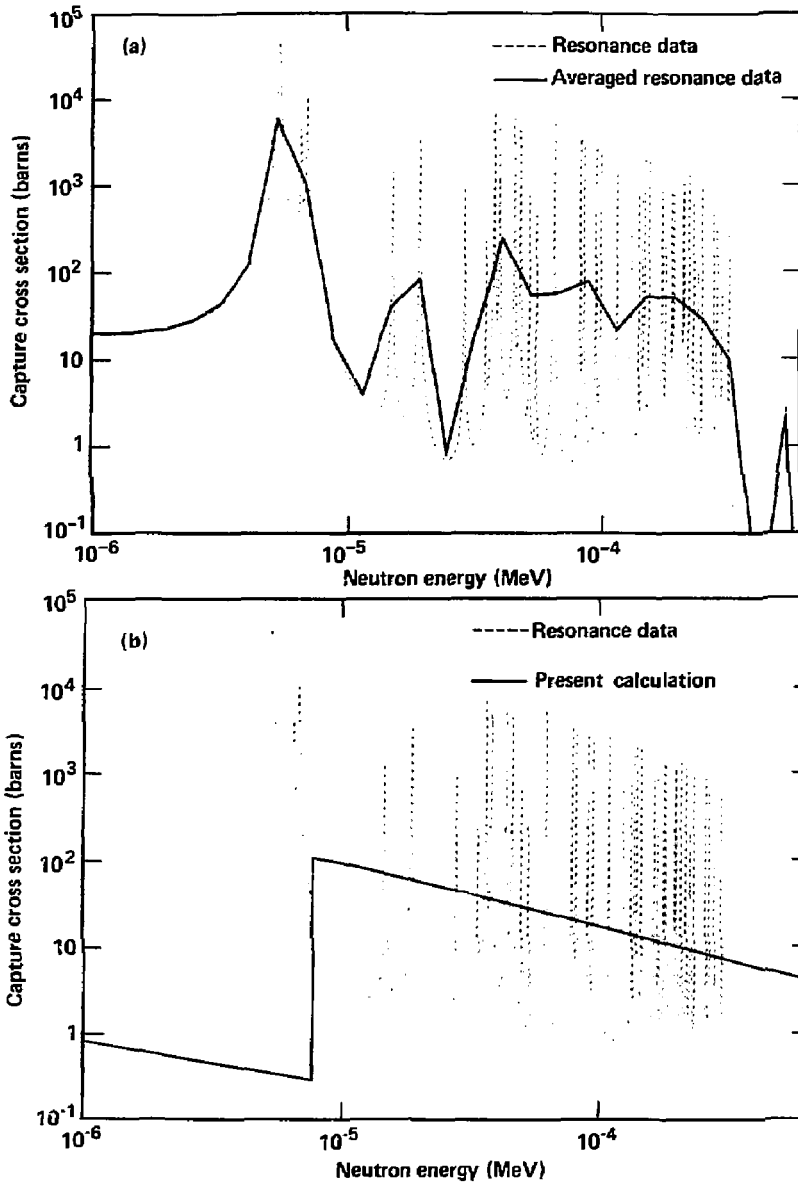


Figure 7. (a) Numerical average through the resonances in the ^{147}Pm neutron-capture excitation function (bound resonances excluded).
 (b) Comparison of data and calculation for the ^{147}Pm neutron-capture excitation function in the resolved-resonance region (bound resonances excluded).

reflect the height of the first resonance, and in this case the estimate is poor. Only if the thermal cross section is known, or if some resonance data have been measured, can we hope to significantly improve this type of estimate. Our $(E_n)^{-1/2}$ extrapolation to thermal energy yields a thermal capture cross section that is too low by a factor of about 30 compared with measurement. Even a resonance integral measurement on some of the presently unmeasured targets would allow us to adjust the magnitude of the $(E_n)^{-1/2}$ portion of each excitation function and, it is hoped, arrive at a more accurate estimate of these low-energy cross sections.

For completeness, we list our calculated neutron-capture excitation function in Table 5.

Using a very simple, systematic approach, Belanova, et al.¹⁷ estimated a number of fission-product cross sections. Their estimates are for the 1-keV to 10-MeV range, and in the case of target ^{147}Pm , their estimate exceeds our calculation by a factor of roughly 3, as does the evaluation of Gruppelaar,¹⁸ which was normalized to an integral measurement. In view of these comparisons, we feel our unadjusted calculations are probably reliable to within a factor of 2.

POSSIBLE CALCULATIONAL IMPROVEMENTS

The most important improvement of the input for our calculations would be more complete sets of discrete levels for the nuclei ^{144}Sm , ^{145}Sm , ^{146}Sm , ^{145}Pm , and ^{146}Pm . This type of effort involves theoretical calculations and estimates to insure that no levels are overlooked, even if they haven't been observed experimentally. The work would require a significant number of man-months by the Nuclear Properties Group of the Nuclear Chemistry Division.

The next problem would be to develop a neutron optical potential (deformed or spherical equivalent) that better represents the samarium-promethium mass region than does our ^{169}Tm potential. Again, this would involve several man-months of effort, plus a large amount of computer time.

Then, we would want to calculate capture cross sections wherever experimental data exist for isotopes of elements from praseodymium to europium, to test our understanding of all of the physics quantities that go

Table 5. Calculated neutron-capture cross sections for ^{147}Pm .

E(MeV)	$\sigma(\text{b})$	E(MeV)	$\sigma(\text{b})$
2.54×10^{-8}	5.18	7.00×10^{-4}	4.15
4.00×10^{-8}	4.12	1.00×10^{-3}	3.13
7.00×10^{-8}	3.12	2.00×10^{-3}	1.90
1.00×10^{-7}	2.61	4.00×10^{-3}	1.22
2.00×10^{-7}	1.84	7.00×10^{-3}	8.86×10^{-1}
4.00×10^{-7}	1.30	1.00×10^{-2}	7.25×10^{-1}
7.00×10^{-7}	9.86×10^{-1}	2.00×10^{-2}	4.81×10^{-1}
1.00×10^{-6}	8.25×10^{-1}	4.00×10^{-2}	3.09×10^{-1}
2.00×10^{-6}	5.83×10^{-1}	7.00×10^{-2}	2.19×10^{-1}
4.00×10^{-6}	4.12×10^{-1}	1.00×10^{-1}	1.68×10^{-1}
7.00×10^{-6}	3.12×10^{-1}	2.00×10^{-1}	1.09×10^{-1}
7.80×10^{-6}	2.95×10^{-1}	4.00×10^{-1}	9.16×10^{-2}
7.90×10^{-6}	1.08×10^2	6.00×10^{-1}	8.87×10^{-2}
1.00×10^{-5}	9.57×10^1	8.00×10^{-1}	9.15×10^{-2}
2.00×10^{-5}	5.97×10^1	1.00	9.63×10^{-2}
4.00×10^{-5}	3.65×10^1	1.25	1.04×10^{-1}
7.00×10^{-5}	2.42×10^1	1.50	1.02×10^{-1}
1.00×10^{-4}	1.85×10^1	2.00	4.59×10^{-2}
2.00×10^{-4}	1.09×10^1	2.50	2.27×10^{-2}
4.00×10^{-4}	6.38		

into our calculations. In a similar way, the resonance regions should be studied to improve the low-energy portions of the neutron-capture cross sections.

We feel, therefore, that it would require a major effort for us to make significant improvements in our present calculations.

ACKNOWLEDGMENT

We are grateful to R. J. Howerton for his assistance with the resonance-region parameters and cross sections of ^{147}Pm .

REFERENCES

1. "Chart of the Nuclides," General Electric Corp., 1984.
2. M. Nurmi, P. Kauranen, and A. Siivola, " Pm^{145} : A New Alpha Activity," Phys. Rev. **127**, 943 (1962).
3. S. F. Mughabghab, Neutron Cross Sections, Vol. 1, Neutron Resonance Parameters and Thermal Cross Sections, Part B: Z = 61 - 100, (Academic Press, New York, 1984), pp. 62-1 to 62-21.
4. W. E. Carey, et al., "Radioactive Sm^{145} and Pm^{145} ," Bull. Am. Phys. Soc., **3**, 63 (1958).
5. R. J. Doyas, et al., An Integrated System for Production of Neutronics and Photonics Calculation Constants, Vol. 5, CLYDE, a Code for the Production of Computational Constants from Nuclear Data, Lawrence Livermore National Laboratory, Livermore, CA, UCRL-50400, Vol. 5 (1971), p. 78.
6. D. G. Gardner, "Methods for Calculating Neutron Capture Cross Sections and Gamma-Ray Spectra," Neutron Radiative Capture, R. E. Chrien, ed., (Pergamon Press, New York, 1984), Chapter III, pp. 62-118.
7. M. Uhl, Acta Phys. Austriaca **31**, 245 (1970).
8. C. L. Dunford, A Unified Model for Analysis of Compound Nucleus Reactions, Atomics International, Canoga Park, CA, AI-AEC-12931 (1970).
9. A. H. Wapstra and K. Bos, "The 1977 Atomic Mass Evaluation," At. Data Nucl. Data **19**, 215 (1977).
10. Table of Isotopes, C. M. Lederer and V. S. Shirley, eds., (John Wiley and Sons, New York, 1978).
11. M. Collin and E. D. Arthur, Determination of 'Equivalent' Spherical Optical-Model Parameters for Neutron Reactions on Thulium Isotopes, Los Alamos National Laboratory, Los Alamos, NM, LA-9647-PR (1982), p. 17.
12. V. N. Kononov, et al., Sov. J. Nucl. Phys. **27** (1), 5 (1978).
13. D. I. Garber and R. R. Kinsey, Neutron Cross Sections, Vol. II, Curves, Brookhaven National Laboratory, Upton, NY, BNL-325 (1976), p. 331.
14. R. J. Howerton, Lawrence Livermore National Laboratory, Livermore, CA private communication (September 1985).
15. D. G. Gardner, M. A. Gardner, and R. W. Hoff, Absolute Dipole Gamma-Ray Strength Functions for ^{176}Lu , UCRL-91098 (1984); Proc. of the Int. Symp. on Capture Gamma-Ray Spectroscopy and Related Topics, 1984, Knoxville, S. Raman, ed., AIP Conf. Proc. #125 (1985), p. 513.

16. J. L. Cook, H. Ferguson, and A. R. Musgrove, Nuclear Level Densities in Intermediate and Heavy Nuclei, AEC/TM 392 (1967).
17. T. S. Belanova, et al., Comparative Analysis of Estimates of Neutron Radiative Capture Cross Sections for the Most Important Fission Products, "SATEAZ 57 (4), 673 (1984).
18. H. Gruppelaar, Status of Recent Fast-Capture-Cross-Section Evaluations for Important Fission Product Nuclides, Argonne National Laboratory, Argonne, IL, ANL-83-4 (1983), p. 473.

JMB/prs